ChemComm

ROYAL SOCIETY OF CHEMISTRY

FEATURE ARTICLE

View Article Online
View Journal | View Issue

Check for updates

Cite this: *Chem. Commun.*, 2023, **59**, 2399

Fluorescence, ultrasonic and photoacoustic imaging for analysis and diagnosis of diseases

Binbin Chu,†[a] Zhiming Chen,†[b] Haoliang Shi,[a] Xiaofeng Wu,[b] Houyu Wang,[a] Fenglin Dong*[b] and Yao He*[a]

Biomedical imaging technology, which allows us to peer deeply within living subjects and visually explore the delivery and distribution of agents in living things, is producing tremendous opportunities for the early diagnosis and precise therapy of diseases. In this feature article, based on reviewing the latest representative examples of progress together with our recent efforts in the bioimaging field, we intend to introduce three typical kinds of non-invasive imaging technologies, *i.e.*, fluorescence, ultrasonic and photoacoustic imaging, in which optical and/or acoustic signals are employed for analyzing various diseases. In particular, fluorescence imaging possesses a series of outstanding advantages, such as high temporal resolution, as well as rapid and sensitive feedback. Hence, in the first section, we will introduce the latest studies on developing novel fluorescence imaging methods for imaging bacterial infections, cancer and lymph node metastasis in a long-term and real-time manner. However, the issues of imaging penetration depth induced by photon scattering and light attenuation of biological tissue limit their widespread *in vivo* imaging applications. Taking advantage of the excellect penetration depth of acoustic signals, ultrasonic imaging has been widely applied for determining the location, size and shape of organs, identifying normal and abnormal tissues, as well as confirming the edges of lesions in hospitals. Thus, in the second section, we will briefly summarize recent advances in ultrasonic imaging techniques for diagnosing diseases in deep tissues. Nevertheless, the absence of lesion targeting and dependency on a professional technician may lead to the possibility of false-positive diagnosis. By combining the merits of both optical and acoustic signals, newly-developed photoacoustic imaging, simultaneously featuring higher temporal and spatial resolution with good sensitivity, as well as deeper penetration depth, is discussed in the third secretion. In the final part, we further discuss the major challenges and prospects for developing imaging technology for accurate disease diagnosis. We believe that these non-invasive imaging technologies will introduce a new perspective for the precise diagnosis of various diseases in the future.

Received 6th December 2022,
Accepted 23rd January 2023

DOI: 10.1039/d2cc06654h

rsc.li/chemcomm

Published on 24 2023. Downloaded on 11/13/2025 12:52:34 PM.

[a] *Suzhou Key Laboratory of Nanotechnology and Biomedicine, Institute of Functional Nano and Soft Materials (FUNSOM), Soochow University, Suzhou, Jiangsu 215123, China. E-mail: yaohe@suda.edu.cn*

[b] *Department of Ultrasound, The First Affiliated Hospital of Soochow University, Suzhou, Jiangsu 215006, China. E-mail: fldong@suda.edu.cn*

† These authors contributed equally to this work.

Binbin Chu

Binbin Chu received his PhD in Chemistry from the Institute of Functional Nano & Soft Materials (FUNSOM) at Soochow University in 2020. He is currently a Postdoctoral Fellow at Soochow University. His research interests mainly focus on designing and constructing silicon nanomaterial-based platforms for the imaging and therapy of diseases, such as cancer, ophthalmic diseases, and bacterial infections.

Zhiming Chen

Zhiming Chen received his BS degree in Radiation Medicine from the College of Radiation Medicine and Protection at Soochow University in 2012. He is now studying for a Master's degree in the First Clinical College of Soochow University. His current research interests focus on the ultrasound diagnosis of diseases.

Published on 24 2023. Downloaded on 11/13/2025 12:52:34 PM.

1. Introduction

Bioimaging techniques enable an in-depth understanding and direct visualization of the pathological changes of diseases in living subjects.[1–5] Since a growing body of evidence indicates the importance of bioimaging technology, numerous kinds of bioimaging technologies, such as computed tomography (CT), single photon emission CT (SPECT), positron emission tomography (PET), X-ray imaging, radiation imaging, Raman imaging, magnetic resonance imaging (MRI), fluorescence imaging, ultrasonic imaging and photoacoustic imaging, have been developed for the diagnosis and determination of diseases in the laboratory, and preclinical and clinical trials.[4–12] Among them, owing to its outstanding advantages of rapid and sensitive feedback, multiple signal acquisition capability, high temporal resolution, as well as maneuverable instruments, the non-invasive fluorescence imaging method has been employed as a powerful tool for labeling and tracing specific molecules, proteins and organelles in living cells and even whole animals, and is hence capable of imaging and monitoring different diseases,[13–19] such as ocular diseases, different bacterial infections, cancer and lymph node (LN) metastasis. Fluorescence imaging can also be utilized to guide surgery in the treatment of disease.[20–22] Numerous previous investigations have indicated that optical signals, which are collected and analyzed in fluorescence imaging, are mainly decided by interactions (including reflection, absorbance and scattering) between photons and biological tissues.[18] However, intrinsic autofluorescence, photon scattering and light attenuation by biological tissues results in a low tissue penetration depth, unfavourable for imaging analysis in deep

Haoliang Shi

Haoliang Shi received his BS degree in Engineering from the College of Nano Science and Technology (CNST) at Soochow University in 2022. Now he is a graduate student in the Institute of functional Nano & Soft Material (FUNSOM) at Soochow University, China. His current research interests focus on the preparation and application of engineered mimicking exosomes in ophthalmology.

Xiaofeng Wu

Xiaofeng Wu received her MD degree in Imaging and Nuclear Medicine from the Jinzhou Medical University in 2016. Currently, she is an attending physician of Department of Ultrasound of the First Affiliated Hospital of Soochow University. She is on the Youth Committee of the Ultrasound Medicine Branch of China Association for the Promotion of International Healthcare Exchange, the Youth Committee of the Suzhou Medical Association Ultrasound Professional Committee and is the Secretary of the Interventional Sub-group. Her research focuses on diagnosis and therapy by interventional ultrasound.

Houyu Wang

Houyu Wang received his PhD degree from Shanghai Jiaotong University in 2013. Currently, he is a research professor in Soochow University. In recent years, his research has focused on the optical detection of infections caused by different bacteria in the body. He has published more than 50 papers in high-quality peer-reviewed journals so far, which were published where he was first author or corresponding author.

Fenglin Dong

Fenglin Dong, associate professor of Soochow University and chief physician, has been in clinical practice for 20 years. He has been the director of the Department of Ultrasound of the First Affiliated Hospital of Soochow University since 2014. Currently, he holds a lot of academic positions, such as Vice President of the Ultrasound Medicine Branch of the China Association for the Promotion of International Healthcare Exchange, Vice President of Jiangsu Medical Doctor Association of Ultrasound. He received Training Object of "Six Talent Peaks" of Jiangsu Province in 2019, "Key talent of Suzhou" in 2022. His research focuses on diagnosis and therapy by interventional ultrasound.

 This journal is © The Royal Society of Chemistry 2023

Published on 24 2023. Downloaded on 11/13/2025 12:52:34 PM.

tissues.[16–18] In contrast, ultrasonic imaging technology features excellent tissue penetration ability, since ultrasound can travel up to centimeters deep into biological tissue without loss of coherence, enabling the feasibility of non-invasive imaging of entire organs and organisms at high spatial (∼100 μm) and temporal resolution (∼1 ms).[23] On this basis, ultrasonic imaging has been widely applied for detecting and diagnosing diseases,[24–28] such as tumors in different organs or tissues (*e.g.*, thyroid, breast, prostate, liver, kidney, and stomach), inflammatory diseases and other types of abnormal situations. Meanwhile, the exploitation of ultrasonic imaging as a guidance method is essential in medical procedures, such as surgery, biopsy and microwave ablation.[29,30] Current ultrasonic imaging technologies mainly include grayscale and Doppler ultrasonography, as well as the contrast-enhanced ultrasonic imaging modality. However, the original ultrasound images show inherent characteristics of low contrast and fuzzy boundaries, which remain challenges for the automatic segmentation of tumors and the professionalism of technicians.[31,32] Furthermore, the absence of a lesion targeting capability is adverse to precisely diagnosing and determining diseases. These above challenges may be addressed by combining the specific features of both optical and acoustic signals into one imaging technology.[33–36] Accumulating evidence shows that the emerging photoacoustic imaging, one kind of hybrid imaging modality which simultaneously takes advantage of both optical and acoustic signals, has been designed and has served as a versatile tool for disease imaging and analysis.[37–39] Many photoacoustic contrast agents have been constructed in recent developments, intended to improve the quality and resolution of images and increase the accuracy of disease diagnosis.[37–39] More recently, emerging bioorthogonal chemistry has emerged as a powerful strategy to design and develop high-performance probes and/or contrast agents (*e.g.*, tetrazine bioorthogonal probes and bispecific immunoconjugate) for wash-free imaging and the early diagnosis of specific biological targets in tumors.[40–44] The achievements of bioorthogonal chemistry in the design and construction of novel probes or contrast agents would provide new opportunities for improving fluorescence, ultrasonic and photoacoustic imaging. In another respect, with the great advances in nanotechnology, the fabrication of functional nanosystems would produce considerable new opportunities for designing and developing high-quality fluorescence, ultrasonic and photoacoustic imaging techniques.[45–48]

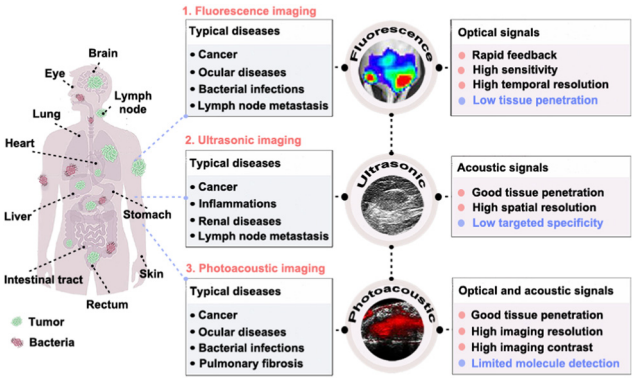

Fig. 1 Scheme of fluorescence, ultrasonic and photoacoustic imaging technology in precise disease detection and diagnosis. Reprinted with permission from ref. 79, 106 and 190. Copyright 2018 Springer Nature; 2022 Wiley-VCH Verlag GmbH & Co. KGaA, Weinheim; 2022 Springer Nature Limited.

Based on the latest representative examples of progress together with our recent efforts, we will survey representative advances in these three typical classes of imaging technology (*i.e.*, fluorescence, ultrasonic and photoacoustic imaging modalities) in this Feature article (as exhibited in Fig. 1). The first section discusses the latest studies for designing and fabricating novel fluorescence imaging strategies with the capability of lesion targeting and crossing biological barriers (*e.g.*, the blood–brain barrier (BBB)), which are further employed for long-term and real-time imaging analysis and detection of bacterial infections, cancer and LN metastasis. The second section explores optimized ultrasonic imaging techniques, and the fabrication of novel ultrasonic contrast agents with improved imaging and targeting ability in contrast-enhanced ultrasonic imaging. The third section discusses emerging approaches for constructing high-performance photoacoustic imaging methods, suitable for accurately diagnosing disease. The final part of this review illustrates conclusions about and future perspectives for fluorescence, ultrasonic and photoacoustic imaging modalities in clinical transformation and disease diagnosis.

Yao He

Yao He is a professor of Soochow University, and serves as the director of Suzhou Key Laboratory of Nanotechnology and Biomedicine. He has authored over 150 SCI papers, with more than 12 000 citations. Prof. He received the First prize of Jiangsu Science and Technology Award in 2017 (Ranking the first), and the Science and Technology Award for Chinese Youth in 2022. He was supported by the National Natural Science Funds for Distinguished Young Youths in 2018. His research focuses on the development of nanotechnology for biomedical applications to provide new powerful tools for the diagnosis and therapy of diseases.

2. Fluorescence imaging

In the fluorescence imaging method, multifunctional probes, simultaneously featuring excellent fluorescent properties (*e.g.*, strong and stable fluorescence, multicolor-emitting fluorescent signals, or near-infrared fluorescence), lesion targeting and accumulation capability, are able to improve the quality and

Published on 24 2023. Downloaded on 11/13/2025 12:52:34 PM.

resolution of images.[16] Numerous kinds of fluorescent probes (*e.g.*, fluorescent proteins, fluorescent dyes and fluorescent nanomaterial-based probes) have been employed to label and trace different molecules, proteins, cells, and tissues and their dynamic progress.[49–58] In particular, fluorescent proteins are suitable for labeling various cells, viruses, genes and so forth; fluorescent dyes are appropriate for imaging and analyzing antibodies, peptides, small molecule drugs and so on. With significant advances in nanotechnology, nanomaterials (*e.g.*, II–VI quantum dots (QDs), carbon dots (CDs), upconverting nanoparticles (UCNPs) and silicon-based nanoparticles (SiNPs)) featuring attractive optical properties, have been exploited as novel high-performance fluorescent nanoprobes for biomedical imaging applications.[59–71] As demonstrated in previous studies, the resultant fluorescent nanomaterials (*e.g.*, II–VI QDs and SiNPs) possess superior fluorescent stability compared to organic dyes, and thus are eminently suitable for the long-term and real-time imaging analysis and detection of diseases.[72–75] Recently, fluorescent SiNPs, porous SiNPs and mesoporous silica NPs (MSNs) have been explored as excellent antibiotics, with highly selective imaging and therapeutic activity against bacteria.[76–78] For example, Zhai *et al.* synthesized a class of theranostic probe, made of vancomycin (Van)-modified fluorescent SiNPs (SiNPs-Van) to specifically image Gram-positive bacteria, such as *Staphylococcus aureus* (*S. aureus*).[79]

As presented in Fig. 2(a), the designed SiNPs-Van probes offered the ability to specifically target and locate on the surface of Gram-positive bacteria, such as *S. aureus*, because the Van on the surface of SiNPs-Van probes can specifically identify the D-Ala-D-Ala Van binding sites on the walls of specific bacteria. Fig. 2(b) further shows that obvious and stable fluorescence signals can be detected in infected sites even after 24 h treatments, while the fluorescence signals of the developed nanoprobes in control sites are almost missing after 9 h treatments. These results revealed that the SiNPs-Van nanoprobes showed longer retention time in infected sites. Further, the fluorescent signals greatly decreased after continuous therapy for 8 days, indicating the therapeutic effects of the SiNPs-Van (Fig. 2(c)). Following that, the same group further exploited the SiNPs-Van probes for rapidly imaging *S. aureus in vitro*, capable of diagnosing *S. aureus*-induced bacterial keratitis in a short time (less than 10 min).[80] On this basis, Tang *et al.* developed a novel SiNP-based nanoprobe, mainly consisting of fluorescent SiNPs functionalized with glucose polymer (GP) molecules and loaded with chlorin e6 (Ce6) agents (GP-Ce6-SiNPs),[81] aiming at concurrent fluorescence imaging and treatments of different bacterial infections (Fig. 2(d)). As exhibited in Fig. 2(e), obvious fluorescence signals, *e.g.*, green fluorescence signals from SiNPs and red fluorescence signals from Ce6, could be detected on both left and right sites infected with 10^7 CFU of *P. aeruginosa* (PA) and *S. aureus* (SA), respectively, revealing the bacterial broad-spectrum imaging capability of the developed GP-Ce6-SiNPs nanoprobes. More importantly, when the bacterial concentration was as low as 10^5 CFU, the fluorescence signals of the SiNPs and Ce6 were still detectable in bacteria-infected sites,

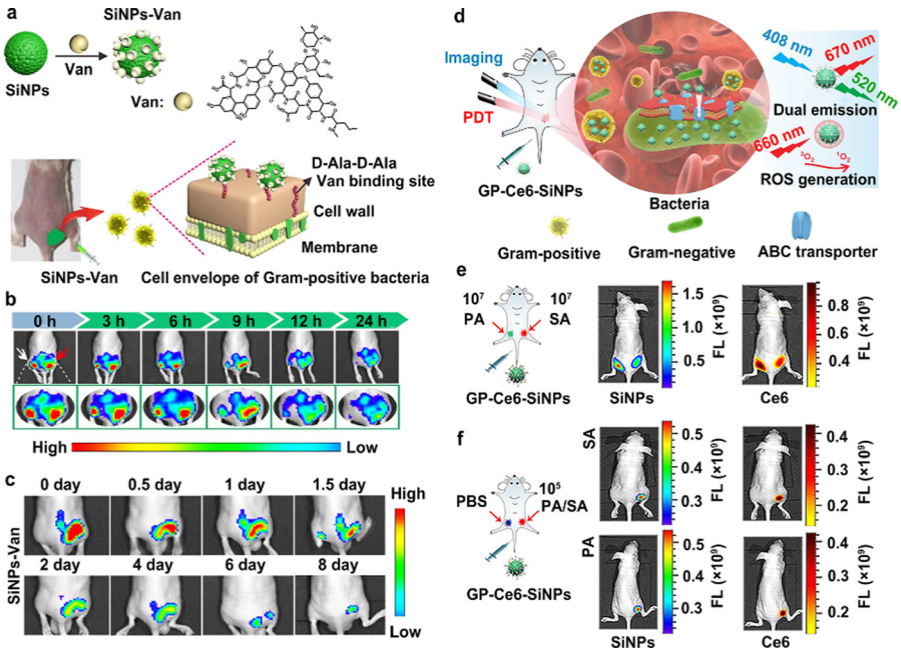

Fig. 2 Fluorescent SiNP-based probes for the sensitive imaging of bacterial infections. (a) A schematic explanation of the preparation of SiNPs-Van for the imaging and treatment of different bacteria. (b) Images of infected and uninfected sites after treatment with SiNPs-Van at different time points. The red arrow indicates infected sites; the white arrow indicates uninfected sites. (c) Images of *S. aureus*-infected mice after treatment with SiNPs-Van for 8 days. Reprinted with permission from ref. 79. Copyright 2018 Springer Nature. (d) A schematic explanation of GP-Ce6-SiNPs developed for imaging and treating different kinds of bacterial infection. (e) Fluorescent images of SA (right) or PA (left) infected sites on the back of mice after treatment with the developed GP-Ce6-SiNPs. The concentration of bacteria was 1.0×10^7 CFU. (f) Fluorescent images of SA or PA (right) and PBS (left) treated sites on the back of mice after treatment with the developed GP-Ce6-SiNPs. The concentration of bacteria was as low as 1.0×10^5 CFU. Reprinted with permission from ref. 81. Copyright 2019 Springer Nature Limited.

 This journal is © The Royal Society of Chemistry 2023

Published on 24 2023. Downloaded on 11/13/2025 12:52:34 PM.

further revealing the highly-sensitive imaging capability of the designed GP-Ce6-SiNPs for various bacteria (Fig. 2(f)). Thus, this research could also provide imaging evidence for discriminating as few as 10^5 CFU of SA or PA *in vivo*.

To target and label specific tumor cells, He and coworkers utilized a kind of cyclo-(Arg-Gly-Asp-D-Tyr-Cys) peptide (namely c(RGDyC)) to make various fluorescent silicon nanomaterials with the function of specific tumor-targeting capability, suitable for the analysis and detection of tumors with overexpressed $\alpha_v\beta_3$ on their surface.[82,83] Further, the c(RGDyC)-modified fluorescent SiNPs (SiNPs-RGD) could also emerge as nanoprobes for the targeted imaging detection of corneal neovascularization (NV) owing to the targeting ability of c(RGDyC) for new blood vessels.[84] As is well known, the blood–brain barrier (BBB) would inhibit the fluorescence imaging by probes for labeling and monitoring glioblastoma (GBM) and brain diseases.[85–87] Hence, the design and fabrication of novel fluorescent nanoprobes featuring outstanding BBB penetrability are of great significance, allowing the *in vivo* imaging analysis and detection of brain diseases.

Previous studies have revealed that bacteria can bypass the specific BBB *in vivo*,[88–90] indicating that bacteria could be employed for the treatment of central nervous system diseases. By taking into account the merits of bacterial systems, Sun and co-workers developed a type of nanobacteria probe (namely Trojan nanobacteria) by combining fluorescent SiNP nanoprobes and live bacteria.[91] The developed Trojan nanobacteria simultaneously possess the optical properties of SiNPs and the BBB penetrability of bacteria, and are therefore suitable for *in vivo* multi-modal imaging and combined therapy of tumors in the brain or deep tissues.[91,92] In 2022, through surface modification with the BBB-targeting ligand glucosamine (G), the same group further developed a kind of nanoprobe with BBB-targeting ability, which was made from G-modified SiNPs loaded with ICG molecules (G-ICG-SiNPs).[93] The G-ICG-SiNPs nanoprobes were able to bypass the BBB through GLUT1-mediated transcytosis because of the existence of G molecules, and are thus capable of simultaneous fluorescence imaging and photothermal therapy of GBM.

Recently-reported studies have revealed that fluorescent nanomaterials encapsulated with different cellular membranes can also obtain distinct targeting ability, allowing *in vivo* imaging and tracing of tumors.[94–96] Han *et al.* thus designed a SiNP-based exosome (SiNPs@EXO) probe through facile electroporation effects (Fig. 3(a)).[97] The developed SiNPs@EXO probes featured homologous targeting capability, as well as strong and stable fluorescence, which was able to distinguish normal and metastatic sentinel lymph nodes (SLNs). In particular, because of the tumor-homing effects of cancer-cell-driven exosomes, the SiNPs@EXO probes could trace a homologous tumor cell and accumulate in metastatic SLNs rather than normal SLNs, thus enabling the identification of normal and metastatic SLNs (Fig. 3(b)). Fig. 3(c) demonstrates that weak fluorescence signals could be detected in the SiNP-treated metastatic SLNs; in sharp contrast, obvious green fluorescence signals could be observed in the metastatic SLNs of a mouse

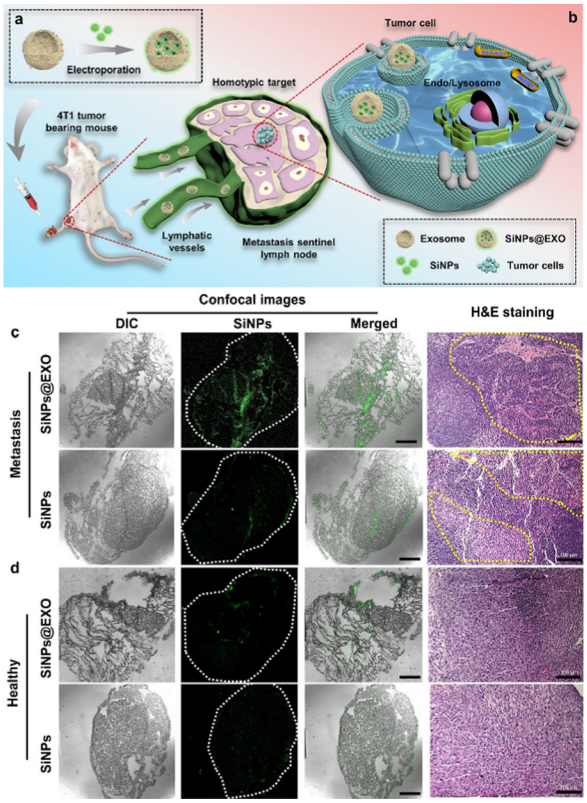

Fig. 3 Fluorescent SiNPs@EXO probes for distinguishing normal and metastatic SLNs. (a) Scheme of preparation of SiNPs@EXO nanoprobes. (b) Scheme of SiNPs@EXO nanoprobes specifically tracing LN metastasis *in vivo*. (c) Confocal and H&E-staining images of metastatic SLN frozen sections after treatment with SiNPs@EXO. Scale bars, 1 mm and 100 μm. (d) Confocal and H&E-staining images of healthy SLN frozen sections after the treatment with SiNPs@EXO. Scale bars, 1 mm and 100 μm. Reprinted with permission from ref. 97. Copyright 2021 American Chemical Society.

with a tumor. Meanwhile, as exhibited in Fig. 3(d), both SiNP- and SiNPs@EXO-treated healthy SLNs showed negligible green fluorescence signals, indicating that SiNPs@EXO probes possessed targeting ability for metastatic SLNs, and are more suitable for distinguishing normal and metastatic SLNs.

Despite the above-mentioned achievements in fluorescence imaging, several limitations, including tissue absorption, scattering and spontaneous fluorescence, are adverse to the resolution of *in vivo* fluorescence imaging.[98] In comparison to fluorescence imaging, phosphorescence imaging can to some extent eliminate interference from biological auto-fluorescence and obtain higher-quality images with a high signal-to-background ratio through time-resolved imaging techniques.[98] In 2020, Wang *et al.* designed a type of silicon-based nanomaterial, made of metal–organic framework (MOF)-modified SiNPs (MOFs@SiNPs), which could exhibit good room-temperature phosphorescence signals (maximum emission wavelength: 505 nm).[99] In the following year, Cui *et al.* developed zinc-doped silica nanospheres (Zn@SiNSs), which simultaneously possessed outstanding fluorescence and room-temperature phosphorescence. Then, they further modified the surface of Zn@SiNSs with functional c(RGDyC) to prepare silicon-based fluorescent and phosphorescent nanoprobes, namely

Published on 24 2023. Downloaded on 11/13/2025 12:52:34 PM.

RGD-Zn@SiNSs probes.[100,101] The as-prepared RGD-Zn@SiNSs probes could distinguish obvious phosphorescence signals from the auto-fluorescence background from tissues. Taking advantage of their unique optical properties and targeting ability, they further employed the newly-constructed RGD-Zn@SiNSs probes for specifically distinguishing tumor tissues from normal tissues.

3. Ultrasonic imaging

Ultrasound, known as a kind of mechanical wave with high penetrative power, has outstanding tissue penetration ability and low side effects on surrounding tissues. In virtue of the high penetration ability of ultrasound, ultrasonic imaging technology has been established as a mature and non-invasive imaging method, suitable for determining the location, size and shape of organs, identifying normal and abnormal tissues, and confirming the edges of lesions in clinics.[102–106] To date, ultrasonic imaging has been one of the most widely-used imaging modalities in hospitals, with tens of millions of patients undergoing ultrasonic examinations each year in China.[107] Commonly-used ultrasonic imaging strategies mainly include grayscale ultrasonic (GSUS), Doppler ultrasonic (DUS), and contrast-enhanced ultrasonic (CEUS) imaging. Among them, GSUS imaging technology, also known as the B-mode ultrasonic imaging modality, is suitable for displaying the anatomical structures of tissues or organs in a section, and further exhibiting the functioning of tissues and organs in a real-time manner.[108] Over past decades, GSUS imaging technology has been widely used to diagnose various diseases in hospitals and clinics.[31,32] While the intrinsic properties of original ultrasonic images, such as low contrast and blurry boundaries, set challenges for the automatic segmentation of tumors.[31,32] Hence, substantial efforts have been made to develop improved ultrasonic imaging methods, including ultrasensitive, quantitative, high-resolution and high-frequency ultrasonic imaging, as well as 4D functional ultrasonic imaging, aimed at improving the accuracy of tumor diagnosis.[109–117] By combination with other image analysis techniques (*e.g.*, artificial intelligence (AI) and deep learning), professionals can reduce interference from false positive signals and effectively determine the boundary of tumor tissues.[31,32,115] In 2017, Dong and co-workers developed an adaptive fuzzy C-means (FCM) method based on the Hausdorff distance definition to segment the ultrasonic imaging of breast cancer by adaptive selection of adjacent regions of each pixel for distance measurement and centroid updating.[31] This suggested that the developed method had the potential for computer-aided diagnosis of breast tumors and other kinds of ultrasound-guided processes. Recently, Fang *et al.* developed a novel type of method for quantifying lung ventilation using a conventional GSUS imaging system.116 They proved that the developed Shannon entropy (namely ShanEn), estimated from an analysis of grayscale histograms of ultrasound images, has great potential to improve the quality of traditional ultrasound lung ventilation detection and provide a quantitative, non-radiation, affordable and bedside monitoring method in future potential applications.

DUS imaging was first proposed by Austrian physicist Christian Doppler in 1842.[118–120] DUS imaging is a physical phenomenon based on the Doppler effect, which is caused by the movement of a sound source or receiver causing a change in the frequency of sound waves (*i.e.*, a Doppler shift). DUS imaging can be divided into pulsed wave,[119] continuous wave,[121] high pulsed repetition frequency,[122] and multi-point selection Doppler,[123] as well as the commonly-used color Doppler flow imaging (CDFI).[124] Because of the high sensitivity of DUS imaging in the detection of moving objects, blood flow information for many organs and parts of the human body can be obtained by DUS imaging technology. In the clinic, DUS examination can be exploited for effectively detecting cerebrovascular diseases, and the timely diagnosis of intracranial and extracranial vascular narrowing obstruction, arteriovenous malformation, and vasospasm. Further, DUS imaging is increasingly utilized to assess renal perfusion in renal diseases, and a Doppler-based renal resistance index can be used to detect patients at risk of acute kidney injury and further distinguish between transient and persistent acute kidney injury. Taking advantage of its high spatio-temporal resolution, deep tissue penetration, as well as high sensitivity and portability, ultrafast DUS imaging technology could provide unique information about brain function through non-invasive imaging analysis.[125]

The CEUS imaging modality has had many types of clinical impact on detection and diagnosis, such as tumors in different tissues (*e.g.*, liver, kidney, uterus, prostate, thyroid, and mammary gland), lymph node metastasis, diverse inflammations, as well as acute kidney injury.[108–115] Compared to GSUS and DUS imaging modalities, the existence of ultrasonic contrast agents in the CEUS imaging method can improve the resolution and sensitivity of ultrasonic diagnosis by enhancing echo-backscatter by the contrast media.[106,126] One kind of commercial ultrasonic contrast agents, *e.g.*, Sonovue, is made of the stabilized MBs where the inert gas (*e.g.*, sulfur hexafluoride (SF6), *etc.*) with low diffusivity, thus featuring good stability and being suitable for the long-term monitoring of each section of diseases.[127–129] Tumor localization using MBs is based on an imaging evaluation of the microvascular perfusion characteristics of abnormal tumors.[130,131] As a typical example, Dong *et al.* combined conventional GSUS and Sonovue-based CEUS imaging modalities, as well as blood cell analysis to improve the diagnostic accuracy for different diseases, such as plasma cell mastitis, malignant small breast masses, and inflammatory mass stage periductal mastitis/duct ectasia.[127–129] In addition, Zlitni *et al.* utilized emerging bioorthogonal reactions and technologies for the highly-selective capture of functionalized MBs to enhance ultrasonic image contrast and improve the quality of ultrasound molecular imaging in the diagnosis of tumors.[44] Nevertheless, these existing MBs (used as established ultrasound contrast agents) are limited to long-term and continuous ultrasonic imaging, being unable to provide integrated information about the occurrence and developments of diseases, due to the insufficient stability and rapid decay of ultrasonic signals of the MBs.[106] To address these issues, Cen *et al.* utilized fluorinated block-bearing amphiphilic copolypeptides to stabilize

 This journal is © The Royal Society of Chemistry 2023

Published on 24 2023. Downloaded on 11/13/2025 12:52:34 PM.

MB-based ultrasonic contrast agents filled with perfluorocarbon (PFC, a commonly-used contrast medium),[132–134] enabling long-term ultrasonic imaging in disease diagnosis.[106] As shown in Fig. 4(a), a series of hydrophilic copolypeptides were synthesized, which were composed of a hydrophilic polyethylene glycol (PEG) block, and fluorinated perfluorooctanoyl and diacetylene moiety blocks, respectively, to induce the formation of outer and inner layers of MB shells. After that, they also emerged as stable materials to stabilize PFC-filled MBs. As further presented in Fig. 4(b), under *in vitro* and *in vivo* conditions, the maleimide moieties on the peripheral surface of PFC-filled MB structures could react with the existing albumin in solution or in bodies, producing *in situ* aggregation to enhance their CEUS imaging capability. They thus indicated their suitability for both GSUS and CEUS imaging of the liver and kidney, accompanied by enhanced CEUS imaging effects.

Benefiting from rapid achievements in the field of functional nanomaterials, numerous kinds of nano-contrast agents, made of functional nanocarriers loaded with gas-releasing molecules or covalently coupled with gas-generating groups,[135] have been designed and constructed in recent years, with potential for GSUS and CEUS imaging analysis. Most previous studies have focused on gases with known anticancer effects, including but not limited to sulfur dioxide (SO_2), hydrogen sulfide (H_2S), nitric oxide (NO), carbon dioxide (CO_2), carbon monoxide (CO), oxygen (O_2), hydrogen (H_2), and heavy gases that act *via* a gas-generating process.[135] Among them, the gases H_2, O_2, CO_2 and nitrogen (N_2) have also emerged as ultrasonic contrast agents, which are feasible for improving the intensity and contrast of acoustic signals in ultrasonic imaging analysis.[136–142] Combined with different nanosystems (*e.g.*, polymers, cerium oxide (CeO_2), ketalized maltodextrin, PLGA NPs and different silicon-based nanomaterials), many kinds of CO_2-generating groups, such as carbonate side chains, ammonium bicarbonate, sodium bicarbonate, and calcium carbonate ($CaCO_3$), have been widely exploited to fabricate novel types of gas-generating nanoplatforms, capable of *in situ* producing MBs of CO_2 gas to enhance the efficiency of ultrasonic imaging analysis.[143–146]

Early in 2010, Kang *et al.* presented a kind of strategy to design and construct novel CO_2 gas-generating polymeric NPs (GGPNPs).[146] They revealed that the GGPNPs could yield nanobubbles that coalesce into microbubbles, which could resonate under an ultrasound field. Thus, the GGPNPs served as contrast agents capable of facilitating *in vivo* ultrasonic imaging. Due to their advantages of good biosafety and easy surface modification, silicon-based nanomaterials, such as dense silica NPs (SiO_2), MSNs and dendritic mesoporous organosilica NPs (MONs), have recently been used to construct gas-generating

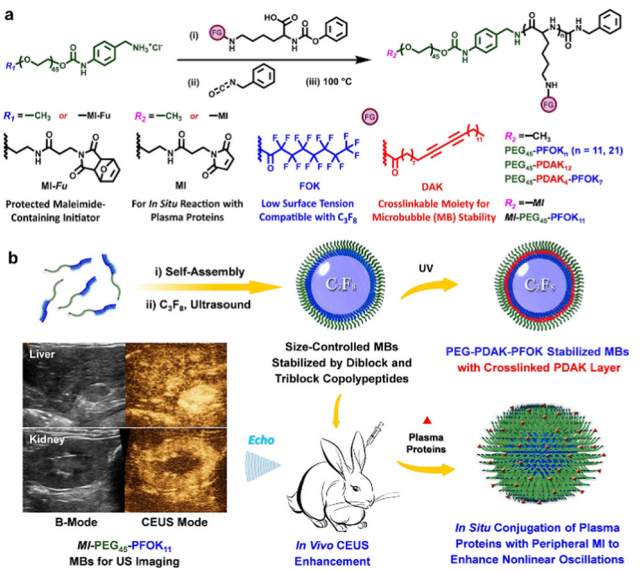

Fig. 4 The construction of ultrasonic contrast agents and their applications in CEUS imaging. (a) Schemes for the preparation of precursors, such as amphiphilic block copolypeptides. (b) Schemes for the fabrication and bioimaging applications of gas-filled MBs *via* ultrasonic treatment. Reprinted with permission from ref. 106. Copyright 2022 Wiley-VCH Verlag GmbH & Co. KGaA, Weinheim.

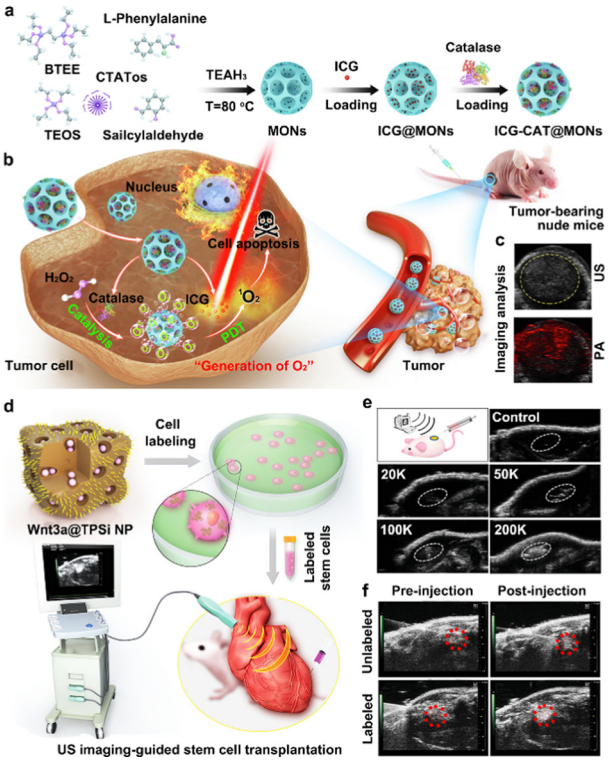

Fig. 5 The construction of silicon-based ultrasonic contrast agents and their CEUS imaging applications. (a) The design and construction of ultrasonic contrast agents of ICG-CAT@MONs. (b) Schematic illustration of ICG-CAT@MONs for dual-modality imaging-guided therapy in an H_2O_2-rich tumor. (c) The ultrasonic and photoacoustic imaging of tumors treated with ICG-CAT@MONs. Reprinted with permission from ref. 140. Copyright 2021 Elsevier B.V. (d) Schematic illustration of the design and preparation of Wnt3a protein-loaded TPSi NPs (Wnt3a@TPSi NPs)-labeled stem cells and their bioimaging applications for guiding the transplantation of stem cells. (e) Ultrasonic images of tissues after the subcutaneous injection of Wnt3a@TPSi NPs-labeled stem cells. (f) *In vivo* ultrasonic imaging of a cardiac structure before and after intramyocardial injection of Wnt3a@TPSi NPs-labeled stem cells. Reprinted with permission from ref. 147. Copyright 2019 Wiley-VCH Verlag GmbH & Co. KGaA, Weinheim.

Published on 24 2023. Downloaded on 11/13/2025 12:52:34 PM.

nanosystems.[139,140] For example, Huang *et al.* designed and developed a novel MON-based ultrasonic contrast agent, made of dendritic MONs simultaneously loaded with indocyanine green (ICG) and the macromolecule catalase (CAT). In this system, the endogenous H_2O_2 would be decomposed by CAT to generate O_2 MBs, and would thus be suitable for intensifying ultrasonic signals in imaging analysis.[140] Fig. 5(a)–(c) illustrate the synthesis of MONs and subsequent loading of ICG and CAT for photoacoustic/ultrasonic dual-modality imaging-guided therapy in H_2O_2-rich tumors.

In addition to gas-releasing systems, aggregations of porous SiNPs have also emerged as ultrasonic contrast agents for enhanced ultrasonic imaging. In 2019, Qi *et al.* presented a new Si-based ultrasonic contrast agent, which consisted of porous Si NPs (TPSi NPs) loaded with Wnt3a protein and coupled with a cell-penetrating peptide (virus-1 transactivator of transcription) (Fig. 5(d)).[147] Fig. 5(e) demonstrates the ultrasonic imaging ability of the developed Wnt3a@TPSi NPs through subcutaneous injection. Furthermore, due to the intracellular aggregation of the TPSi NPs, the designed Wnt3a@TPSi NPs-labeled mesenchymal stem cells (MSCs) could show enhanced acoustic signals, compared to unlabeled MSCs (Fig. 5(f)). This new strategy thus provides a useful reference for exploring the design and construction of non-gas-related ultrasonic contrast agents, *e.g.*, solid ultrasonic contrast agents featuring acoustic scattering, in the clinic.

4. Photoacoustic imaging

As mentioned above, major challenges still remain for improving the tissue penetration of the fluorescent imaging technique, and the specific targeting ability of the ultrasonic imaging method. The emerging photoacoustic imaging, by a combination of both optical and acoustic signals,[37–39] simultaneously features higher temporal and spatial resolution with good sensitivity, deeper penetration depth, and desirable targeting capability. Extensive studies have demonstrated that the acoustic signals generated by the thermal expansion of optically absorbent objects are able to overcome the significant drawbacks of the high scattering of photons in biological tissues.[148,149] In detail, the absorbed light energy can lead to the production of instant thermoelastic expansion in tissue structures, and further create an ultrasound wave with broadband features.[150] Then, the ultrasound wave would be first received through an ultrasonic transducer, and then converted to electric signals, finally yielding a photoacoustic image.[150] The light-absorption coefficient (LOC) of targeted tissues and applied photoacoustic contrast agents can determine the final imaging quality. Hence, after the demonstration of photoacoustic effects by Alexander Graham Bell,[151] many efforts have been devoted to developing high-performance photoacoustic contrast agents, including inorganic (*e.g.*, gold nanomaterials, MXene-based nanomaterials, carbon nanomaterials, and SiNPs) and organic (*e.g.*, organic small molecules, polymers and DNA-derived structures) contrast agents.[152–156] Up to the present, a number of studies have reported the development of photoacoustic contrast agents for the imaging analysis and detection of bacterial infections, tumors, ophthalmic diseases, pulmonary fibrosis, gastrointestinal tract, vasculature, and brain.[154]

Gold nanomaterials and/or nanocomposites, including gold NPs (AuNPs), gold NRs (AuNRs), gold nanostars (AuNSs), gold nanoflowers (AuNFs), gold nanotriangles (AuNTs) and other nanohybrid structures, have been synthesized and exploited to construct photoacoustic contrast agents for the imaging of diseases, since they possess outstanding light absorption and photothermal conversion ability, resulting from significant localized surface plasmon resonance (LSPR) effects.[157–162] Additionally, gold nanomaterials have good physiochemical properties, strong chemical inertness and a high extinction coefficient, as well as a high photothermal conversion effect upon irradiation by a laser source.[163–165] Combined with SiNRs, SiNWs, magnetic NPs (Fe_3O_4 NPs) and bacteria-derived natural Fe_3O_4 magnetosomes, gold nanomaterials have emerged as satellites to form core–satellite nanostructures with specific functionalities.[82,166–168] He and co-workers developed Si–Au nanocomposites with nuclear–satellite structures, *i.e.*, AuNP-decorated SiNRs (Au@SiNRs).[82] As illustrated in Fig. 6(a), the SiNRs with strong and stable fluorescence were first synthesized through a microwave-assisted method, and then the Au@SiNRs were obtained after the *in situ* growth of AuNPs on their surface. The TEM images in Fig. 6(b) show that a number of AuNPs were observed on the surface of a single SiNR. Afterwards, Au@SiNRs-based contrast agents were modified with RGD, enabling their enhanced tumor accumulation. As a result, compared with insignificant or weak photoacoustic signals in the PBS- or Au@SiNRs-treated tumors, more obvious PA signals could be detected in RGD-Au@SiNRs-treated tumors (Fig. 6(c)), providing imaging evidence that the Au@SiNRs were superbly capable of the specific photoacoustic imaging analysis of tumors. Moreover, by including the merits of the good fluorescence performance of SiNRs, the obtained Au@SiNRs probes could be suitable for the multi-modal imaging (*e.g.*, fluorescence and photoacoustic imaging) of tumor tissues. By wrapping the surface of gold nanomaterials with distinctively functional shells, such as chitosan, graphene oxide (GO), silica (SiO_2) or polydopamine (PDA, a robust synthetic melanin), gold core–shell nanostructures can also be designed and constructed.[162,169–171] In particular, owing to the ability of SiO_2 layers to reduce thermal resistance at a particle's surface and stabilize a particle's shape, different kinds of Au–SiO_2 core–shell nanostructures have been fabricated to enhance the photoacoustic response from gold nanomaterials.[170–173] Recent studies highlighted that the thermal expansion of SiO_2-coated nanorods and surrounding liquid could generate an acoustic emission. The enhancement of the thermal conductance between Au–SiO_2 and SiO_2–water interfaces may induce an enhancement in acoustic signals.[170–173] In addition, owing to the targeting ability of hyaluronic acid (HA) for the CD44 receptor (overexpressed on a tumor cell surface),[161,174] HA-modified nanoparticles have been employed to enhance the delivery of drugs, proteins or genes. Based on the advantages of

 This journal is © The Royal Society of Chemistry 2023

Published on 24 2023. Downloaded on 11/13/2025 12:52:34 PM.

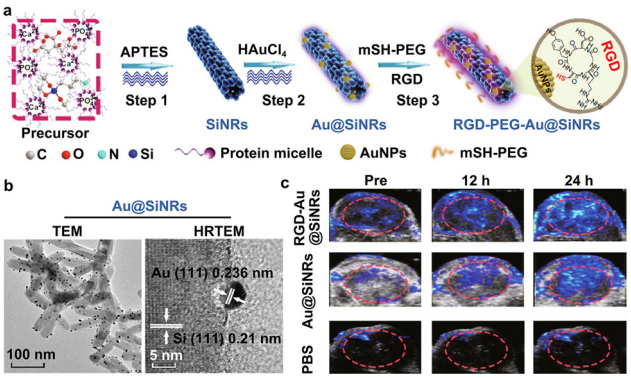

Fig. 6 The construction and photoacoustic imaging analysis of gold nanohybrid-photoacoustic contrast agents. (a) Schemes for the preparation of Au@SiNRs and RGD-Au@SiNRs. (b) TEM images of Au@SiNRs. Scale bars, 100 nm and 5 nm. (c) *In vivo* photoacoustic imaging of tumor tissues treated with the prepared RGD-Au@SiNRs. Reprinted with permission from ref. 82. Copyright 2019 Springer Nature Switzerland AG.

HA, Au–HA nanocomposites have been developed for the photoacoustic targeted imaging of tumors. In addition, metal-related shells (*e.g.*, Ag_2S/Se, Ag, or Pd) are also employed to coat gold nanomaterials for enhanced photoacoustic imaging.[160,175,176] Previous studies revealed that the existence of Ag^+ offers the ability to quench the photoacoustic signals of gold-based contrast agents, while the photoacoustic signals will recover when the Ag^+ ions are released from the surface of the gold-based contrast agents, and thus they are suitable for the selective photoacoustic tracing of Ag^+ release in Ag^+-related bacterial treatments.[160] Furthermore, Pd-tipped Au nanorods (PTA NRs) and Pd-coated Au nanorods (PCA NRs) were also fabricated and used as photoacoustic contrast agents.[175] STEM and element mapping images revealed the successful fabrication of PTA NRs and PCA NRs. After 4 h injection, photoacoustic signals are distinctly enhanced since the distribution of PTA NRs is distinctly increased in the tumor microvasculature; after the treatments for 12 h, the photoacoustic images of the PTA NRs-treated tumor tissues exhibited the strongest enhancement, thus suggesting the long-term blood circulation of PTA NR.

To date, various kinds of strategies have been developed to design multi-functional gold nanoclusters or nanoaggregates, enabling the possibility of enhanced photoacoustic imaging.[177–183] Xu *et al.* presented a simple and versatile approach, combined with emulsion-templated and polymer-guided assembly, to fabricate a series of tuneable gold patterns.[184] The developed gold nanoaggregates are useful for imaging-guided cancer therapy, owing to their longer residence time in tumors. Additionally, other nanomaterials, including nanogels, UCNPs, down-conversion NPs (DCNP) and Ag_2S QDs, have been utilized to prepared spherical AuNPs/AuNRs vesicles by self-assembly.[180–183] In 2017, Emelianov and co-workers used poly(*n*-isopropylacrylamide) (PNIPAM)-based nanogels to control the aggregation of AuNRs,[183] intending to synthesize spherical AuNR nanoclusters with increasing photoacoustic signals. Gao *et al.* developed pH-responsive AuNPs–Ag_2S vesicles, made from the self-assembly of the pH-responsive polymer thiolated polystyrene-*co*-poly(4-vinylpyridine) grafted AuNPs and Ag_2S QDs, which are feasible for multimodal imaging analysis (including photoacoustic and NIR-II fluorescence imaging) of cancer.[181] In 2021, Zhang *et al.* designed a new kind of silica-encapsulated self-assembled gold nanochain (AuNCs@SiO_2), which is suitable for tumor diagnosis in an accurate manner.[179] The SiO_2 shell was formed to improve the biocompatibility and to preserve the physicochemical stability of the AuNC-based contrast agents.

On the other hand, novel strategies for *in situ* AuNP aggregation triggered by internal or external stimuli have been developed. The internal stimuli mainly include cells and their microenvironments, such as immune cells, reactive oxygen species (ROS), proteins, glutathione (GSH), enzymes (*e.g.*, caspase-3 enzyme) and pH.[185–189] The external stimuli consist of drugs or agents (*e.g.*, vascular disrupting agents), chemiluminescence, and ultraviolet light.[190–193] For internal stimuli, Emelianov and co-workers developed a new kind of photoacoustic contrast agent, made of glycol-chitosan-coated gold NPs (GC-AuNPs), realizing the noninvasive imaging of sentinel LN (SLN) metastases.[185] In this case, after peritumoral injection, the injected GC-AuNPs could first be taken up by immune cells and further triggered to form aggregations inside them. Afterwards, the GC-AuNPs-labelled immune cells could be transported to SLNs by lymphatic vessels. Lastly, the existence of a metastatic lesion was able to influence the distribution of GC-AuNPs-labelled immune cells. It has been elucidated that a metastatic lesion could induce a decrease in immune cells in an SLN. Hence, the reduction in photoacoustic signals was exploited to detect SLN metastases *via* ultrasound-guided photoacoustic images. Recent studies have reported that ultraviolet (UV) light is able to trigger the aggregation of small-sized AuNPs.[190–193] Typically, in 2016, Gao *et al.* modified the surface of AuNPs with PEG5000 ligands containing specific diazirine terminal groups, sensitive to 405 nm UV light, to construct photolabile AuNP-based contrast agents, namely PEG–AuNPs.[192] After irradiation by a 405 nm laser, the constructed PEG–AuNPs probes could get together to form larger AuNP aggregations through covalent cross-linking of diazirine groups between the surfaces of two adjacent AuNPs. The results presented in this research demonstrated that the UV-triggered AuNP aggregates were able to exhibit obviously enhanced PA signals, while the primary PEG–AuNPs without irradiation by a UV laser displayed weak photoacoustic signals. On this basis, He and coworkers designed and constructed a novel AuNP-based probe (named GP-dAuNPs@Ce6), made of GP- and diazirine-coupled AuNPs loaded with Ce6 molecules, capable of being eaten by Gram-negative and Gram-positive bacteria, which further aggregated inside the bacterial cells after irradiation by a 405 nm UV laser.[190] As shown in Fig. 7(a), both Gram-negative and Gram-positive bacteria could actively swallow the prepared counterfeit "foods", the GP-dAuNPs@Ce6 probes containing GP groups on their surface, through the bacteria-specific ABC transporter pathway. Importantly, continuous irradiation by the 405 nm laser could induce the *in situ* aggregation of the GP-dAuNPs@Ce6 probes inside the bacteria.

Then, the aggregation of GP-dAuNPs@Ce6 could show significantly enhanced photoacoustic and fluorescent signals, and thus be suitable for multimodal imaging (*e.g.*, fluorescence and photoacoustic imaging). The TEM images in Fig. 7(b)

Published on 24 2023. Downloaded on 11/13/2025 12:52:34 PM.

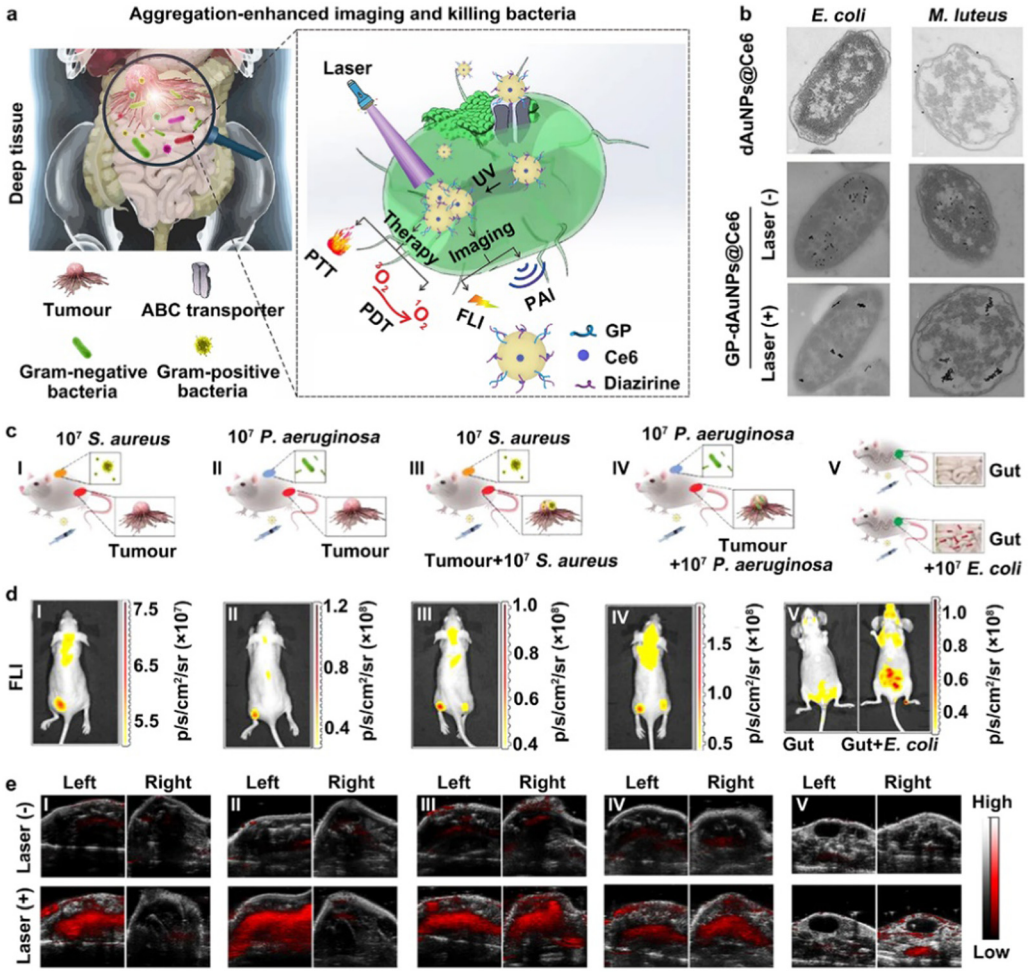

Fig. 7 The construction of AuNP-based contrast agents for the aggregation-enhanced imaging of bacteria. (a) The construction, bacterial targeting and *in situ* UV-induced aggregations of GP-dAuNPs@Ce6 contrast agents. (b) TEM images of *E. coli* and *M. luteus* bacteria treated with GP-dAuNPs@Ce6 with or without UV irradiation. (c) The construction of mouse models with different bacterial infections. (d) The FL imaging analysis of GP-dAuNPs@Ce6-labelled mouse models. (e) The PA imaging analysis of GP-dAuNPs@Ce6-labelled mouse models with or without the irradiation by a 405 nm UV laser. Reprinted with permission from ref. 190. Copyright 2022 Springer Nature Limited.

provide further direct evidence to demonstrate the successful construction of GP-dAuNPs@Ce6 and their UV-induced aggregation ability. To further verify the possibility of multimodal imaging, different models, including bacterial skin infections, intratumoral bacteria, and peritonitis, were constructed. Fig. 7(c)–(e) show that obvious fluorescent signals of Ce6 and enhanced photoacoustic signals of aggregated AuNPs after the irradiation by UV light could be observed in bacteria-rich parts; in comparison, weak fluorescent and photoacoustic signals were detected in the non-bacterial sites. These results proved that the UV-triggered aggregation method would make small-sized AuNPs more feasible for photoacoustic imaging.

5. Conclusions

In summary, we have reviewed representative examples of the developments and recent advances in fluorescence, ultrasonic and photoacoustic imaging for disease detection and diagnosis. As discussed in the above sections, fluorescence imaging possesses significant merits, including rapid and sensitive feedback, the ability to acquire multiple signals, high temporal resolution, as well as manoeuvrable instruments, and is thus suitable for the rapid and sensitive imaging detection of diseases in a real-time manner; ultrasonic imaging has excellent deep tissue penetration, so it is capable of diagnosing diseases in deep tissues; photoacoustic imaging, simultaneously featuring the advantages of optical and acoustic signals, has shown high promise for the detection and diagnosis of different diseases, with high imaging contrast and resolution, as well as specific targeting capability. Although there have been significant achievements in the developments of fluorescence, ultrasonic and photoacoustic imaging technologies, there are still several major challenges at present. For example, while different kinds of probes and contrast agents have recently been developed for bioimaging applications, the reproducible and mass production of these materials is challenging, which is of crucial importance for their widespread applications. On the other hand, considering that identifiable

 This journal is © The Royal Society of Chemistry 2023

Published on 24 2023. Downloaded on 11/13/2025 12:52:34 PM.

targets may also be expressed to some extent in normal cells or tissues, multiple-targeting probes and contrast agents should be exploited to improve the detection specificity of diseases, which is particularly important for a complicated *in vivo* environment. Moreover, for wide-ranging and potential clinical applications, reliable and systematic biosafety assessment of probes and contrast agents, covering *in vitro* and *in vivo* levels, is essentially required. We believe that accompanied by a growing understanding of the above challenges, these biomedical imaging methods would serve as powerful tools and raise new perspectives for the precise analysis and detection of various diseases in the future.

Author contributions

B. B. C. and Z. M. C. contributed equally to this work. B. B. C., Z. M. C., H. L. S., X. F. W. and H. Y. W. completed the investigation and classification of the corresponding literatures. B. B. C., Z. M. C., F. L. D. and Y. H. conceptualized the topic of this review, prepared the scheme. B. B. C. and Z. M. C. prepared the Figures and wrote the draft. F. L. D. and Y. H. gave support during the manuscript preparation, and revised the final draft.

Conflicts of interest

There are no conflicts to declare.

Acknowledgements

The authors acknowledge financial support from the National Natural Science Foundation of China (No. 21825402, 22074101 and 22204117), Natural Science Foundation of Jiangsu Province of China (No. BK20191417), the China Postdoctoral Science Foundation (No. 2021M692347) and the Program for Jiangsu Specially-Appointed Professors to Prof. Yao He, a project funded by the Priority Academic Program Development of Jiangsu Higher Education Institutions (PAPD), 111 Project as well as the Collaborative Innovation Center of Suzhou Nano Science and Technology (NANO-CIC).

Notes and references

1 R. Weissleder, *Nat. Biotechnol.*, 2001, 316–317.
2 X. F. Lin, H. Zhu, Y. Hong and Z. Yang, *Chem. Res. Chin. Univ.*, 2013, **34**, 2139–2145.
3 X. Michalet, F. F. Pinaud, L. A. Bentolila, J. M. Tsay, S. Doose, J. J. Li, G. Sundaresan, A. M. Wu, S. S. Gambhir and S. Weiss, *Science*, 2005, **307**, 538–544.
4 L. L. Chen, L. Zhao, Z. G. Wang, S. L. Liu and D. W. Pang, *Small*, 2022, **18**, 2104567.
5 V. P. Nguyen, T. Zhu, J. Henry, W. Zhang, X. Wang and Y. M. Paulus, *Photonics*, 2022, **9**, 201.
6 Z. Li, Y. Wang, J. Liu, P. Rawding, J. Bu, S. Hong and Q. Hu, *Adv. Mater.*, 2021, **33**, 2102580.
7 J. I. Scott, S. Gutkin, O. Green, E. J. Thompson, T. Kitamura, D. Shabat and M. Vendrell, *Angew. Chem., Int. Ed.*, 2021, **60**, 5699–5703.
8 X. Lu, H. Wang and Y. He, *Chin. J. Chem.*, 2022, **40**, 734–745.
9 C. Zhao, Q. Wang, X. Tao, M. Wang, C. Yu, S. Liu, M. Li, X. Tian, Z. Qi, J. Li, F. Yang, L. Zhu, X. He, X. Zeng, Y. Jiang and M. Yang, *Eur. Radiol.*, 2021, **31**, 3542–3552.
10 L. Zhu, R. Huang, M. Li, Q. Fan, X. Zhao, X. Wu and F. Dong, *Ultrasound Med. Biol.*, 2022, **48**, 1441–1452.
11 J. Liu, X. Wang, M. Hu, Y. Zheng, L. Zhu, W. Wang, J. Hu, Z. Zhou, Y. Dai and F. Dong, *Front. Oncol.*, 2022, **12**, 963925.
12 H. Jin, X. Jiang, Z. Sun and R. Gui, *Coord. Chem. Rev.*, 2021, **431**, 213694.
13 C. Wu, B. Bull, C. Szymanski, K. Christensen and J. McNeill, *ACS Nano*, 2008, **2**, 2415–2423.
14 K. Li and B. Liu, *Chem. Soc. Rev.*, 2014, **43**, 6570–6597.
15 E. A. Owens, M. Henary, G. El Fakhri and H. S. Choi, *Acc. Chem. Res.*, 2016, **49**, 1731–1740.
16 M. Gao, F. Yu, C. Lv, J. Choo and L. Chen, *Chem. Soc. Rev.*, 2017, **46**, 2237–2271.
17 J. Zhao, J. Chen, S. Ma, Q. Liu, L. Huang, X. Chen, K. Lou and W. Wang, *Acta Pharm. Sin. B*, 2018, **8**, 320–338.
18 C. Li, G. Chen, Y. Zhang, F. Wu and Q. Wang, *J. Am. Chem. Soc.*, 2020, **142**, 14789–14804.
19 S. Li, F. Huo and C. Yin, *Chem. Commun.*, 2022, **58**, 12642–12652.
20 A. L. Vahrmeijer, M. Hutteman, J. R. van der Vorst, C. J. H. van de Velde and J. V. Frangioni, *Nat. Rev. Clin. Oncol.*, 2013, **10**, 507–518.
21 E. M. Sevick-Muraca, *Annu. Rev. Med.*, 2012, **63**, 217–231.
22 Q. T. Nguyen, E. S. Olson, T. A. Aguilera, T. Jiang, M. Scadeng, L. G. Ellies and R. Y. Tsien, *Proc. Natl. Acad. Sci. U. S. A.*, 2010, **107**, 4317–4322.
23 Y. Li, R. Lin, C. Liu, J. Chen, H. Liu, R. Zheng, X. Gong and L. Song, *J. Biophotonics*, 2018, **11**, e201800034.
24 P. G. Griffin and O. J. Ginther, *J. Anim. Sci.*, 1992, **70**, 953–972.
25 K. K. Shung, *J. Med. Ultrasound*, 2009, **17**, 25–30.
26 J. R. Cook, R. R. Bouchard and S. Y. Emelianov, *Biomed. Opt. Express*, 2011, **2**, 3193–3206.
27 H. Yang, X. Shen, J. Yan, X. Xie, Z. Chen, T. Li, S. Li, X. Qin, C. Wu and Y. Liu, *Biomater. Sci.*, 2018, **6**, 2426–2439.
28 J. Zhang, L. Song, S. Zhou, M. Hu, Y. Jiao, Y. Teng, Y. Wang and X. Zhang, *RSC Adv.*, 2019, **9**, 35345–35355.
29 A. Bychkov, V. Simonova, V. Zarubin, E. Cherepetskaya and A. Karabutov, *Appl. Sci.*, 2018, **8**, 1931.
30 T. A. Whittingham, *Br. J. Radiol.*, 1997, **70**, S119–S132.
31 Y. Feng, F. Dong, X. Xia, C.-H. Hu, Q. Fan, Y. Hu, M. Gao and S. Mutic, *Med. Phys.*, 2017, **44**, 3752–3760.
32 X. Wu, L. Zhang, J. Sun, Y. Huang, E. Yu, D. Gu, W. Wang, M. Sun, K. Wang, J. Wang, M. Hu, M. Zhou, J. Liu and F. Dong, *Gland Surg.*, 2021, **10**, 1736–1743.
33 X. Zhou, Y. Fang, V. Wimalasiri, C. I. Stains and E. W. Miller, *Chem. Commun.*, 2022, **58**, 11941–11944.
34 A. Qu, L. Xu, C. Xu and H. Kuang, *Chem. Commun.*, 2022, **58**, 12782–12802.
35 J. Chen, Y. Fang, L. Sun, F. Zeng and S. Wu, *Chem. Commun.*, 2020, **56**, 11102–11105.
36 H. Li, J. Wang, P. Wang, J. Zheng, F. Song, T. Yin, G. Zhou, R. Zheng and C. Zhang, *Chem. Commun.*, 2014, **50**, 15163–15166.
37 P. J. Chen, S. H. Hu, C. T. Fan, M. L. Li, Y. Y. Chen, S. Y. Chen and D. M. Liu, *Chem. Commun.*, 2013, **49**, 892–894.
38 P. Beard, *Interface Focus*, 2011, **1**, 602–631.
39 C. Li, C. Liu, Y. Fan, X. Ma, Y. Zhan, X. Lu and Y. Sun, *RSC Chem. Biol.*, 2021, **2**, 743–758.
40 S. L. Scinto, D. A. Bilodeau, R. Hincapie, W. Lee, S. S. Nguyen, M. Xu, C. W. am Ende, M. G. Finn, K. Lang, Q. Lin, J. P. Pezacki, J. A. Prescher, M. S. Robillard and J. M. Fox, *Nat. Rev. Dis. Primers*, 2021, **1**, 30.
41 H. Luo, R. Hernandez, H. Hong, S. A. Graves, Y. Yang, C. G. England, C. P. Theuer, R. J. Nickles and W. Cai, *Proc. Natl. Acad. Sci. U. S. A.*, 2015, **112**, 12806–12811.
42 W. Mao, J. Tang, L. Dai, X. He, J. Li, L. Cai, P. Liao, R. Jiang, J. Zhou and H. Wu, *Angew. Chem., Int. Ed.*, 2021, **60**, 2393–2397.
43 W. Mao, W. Chi, X. He, C. Wang, X. Wang, H. Yang, X. Liu and H. Wu, *Angew. Chem., Int. Ed.*, 2022, **61**, e202117386.
44 A. Zlitni, N. Janzen, F. S. Foster and J. F. Valliant, *Angew. Chem., Int. Ed.*, 2014, **53**, 6459–6463.
45 K. Yang, S. Zhang, J. He and Z. Nie, *Nano Today*, 2021, **36**, 101046.
46 A. A. Hafez, A. Salimi, Z. Jamali, M. Shabani and H. Sheikhghaderi, *Inorg. Nano-Met. Chem.*, 2022, 1–19.

Published on 24 2023. Downloaded on 11/13/2025 12:52:34 PM.

47 N. Wu, C. H. Fan and C. K. Yeh, *Drug Discovery Today*, 2022, **27**, 1590–1603.
48 W. Fan, B. Yung, P. Huang and X. Chen, *Chem. Rev.*, 2017, **117**, 13566–13638.
49 M. Deng, J. Yuan, H. Yang, X. Wu, X. Wei, Y. Du, G. Wong, Y. Tao, G. Liu, Z. Jin and J. Chu, *ACS Nano*, 2021, **15**, 17602–17612.
50 P. Guerra, L. A. Vuillemenot, B. Rae, V. Ladyhina and A. Milias-Argeitis, *ACS Synth. Biol.*, 2022, **11**, 1129–1141.
51 M. Hirano, R. Ando, S. Shimozono, M. Sugiyama, N. Takeda, H. Kurokawa, R. Deguchi, K. Endo, K. Haga, R. Takai-Todaka, S. Inaura, Y. Matsumura, H. Hama, Y. Okada, T. Fujiwara, T. Morimoto, K. Katayama and A. Miyawaki, *Nat. Biotechnol.*, 2022, **40**, 1132–1142.
52 Y. Sun, P. Sun, Z. Li, L. Qu and W. Guo, *Chem. Soc. Rev.*, 2022, **51**, 7170–7205.
53 H. Li, Y. Kim, H. Jung, J. Y. Hyun and I. Shin, *Chem. Soc. Rev.*, 2022, **51**, 8957–9008.
54 C. S. Abeywickrama, *Chem. Commun.*, 2022, **58**, 9855–9869.
55 A. Lesiak, K. Drzozga, J. Cabaj, M. Bański, K. Malecha and A. Podhorodecki, *Nanomaterials*, 2019, **9**, 192.
56 S. Wilhelm, *ACS Nano*, 2017, **11**, 10644–10653.
57 K. P. Loh, D. Ho, G. N. C. Chiu, D. T. Leong, G. Pastorin and E. K. H. Chow, *Adv. Mater.*, 2018, **30**, 1802368.
58 L. Li, Y. Huang, P. Zhao, H. Miao and T. Zhao, *Chem. Res. Chin. Univ.*, 2020, **36**, 955–961.
59 H. Wang and Y. He, *Sensors*, 2017, **17**, 268.
60 H. Liu, W. Zhong, X. Zhang, D. Lin and J. Wu, *J. Mater. Chem. B*, 2021, **9**, 7878–7908.
61 X. Li, Y. Zhang, G. Liu, Z. Luo, L. Zhou, Y. Xue and M. Liu, *RSC Adv.*, 2022, **12**, 7635–7651.
62 I. Zare, M. T. Yaraki, G. Speranza, A. H. Najafabadi, A. Shourangiz-Haghighi, A. B. Nik, B. B. Manshian, C. Saraiva, S. J. Soenen, M. J. Kogan, J. W. Lee, N. V. Apollo, L. Bernardino, E. Araya, D. Mayer, G. Mao and M. R. Hamblin, *Chem. Soc. Rev.*, 2022, **51**, 2601–2680.
63 A. Haddar, E. Ben Ayed, A. Sila, J. L. Putaux, A. Bougatef and S. Boufi, *RSC Adv.*, 2021, **11**, 38990–39003.
64 S. Mourdikoudis, R. M. Pallares and N. T. K. Thanh, *Nanoscale*, 2018, **10**, 12871–12934.
65 M. Cao, Y. Sun, M. Xiao, L. Li, X. Liu, H. Jin and H. Pei, *Chem. Res. Chin. Univ.*, 2020, **36**, 254–260.
66 H. Huang and J. F. Lovell, *Adv. Funct. Mater.*, 2017, **27**, 1603524.
67 X. Fu, H. Bai, F. Lyu, L. Liu and S. Wang, *Chem. Res. Chin. Univ.*, 2020, **36**, 237–242.
68 A. Kumar, S. Kim and J. M. Nam, *J. Am. Chem. Soc.*, 2016, **138**, 14509–14525.
69 X. Huang, Y. Liu, B. Yung, Y. Xiong and X. Chen, *ACS Nano*, 2017, **11**, 5238–5292.
70 B. Chu, A. Wang, L. Cheng, R. Chen, H. Shi, B. Song, F. Dong, H. Wang and Y. He, *J. Nanobiotechnol.*, 2021, **19**, 187.
71 J. Yao, M. Yang and Y. Duan, *Chem. Rev.*, 2014, **114**, 6130–6178.
72 F. Peng, Y. Su, Y. Zhong, C. Fan, S. T. Lee and Y. He, *Acc. Chem. Res.*, 2014, **47**, 612–623.
73 F. Peng, Z. H. Cao, X. Y. Ji, B. B. Chu, Y. Y. Su and Y. He, *Nanomedicine*, 2015, **10**, 2109–2123.
74 B. Chu, H. Wang and Y. He, *Chem. Res. Chin. Univ.*, 2021, **37**, 880–888.
75 B. Chu and Y. He, *Chem. J. Chin. Univ.*, 2022, **43**, 20220546.
76 C. Y. Wang, P. Makvandi, E. N. Zare, F. R. Tay and L. N. Niu, *Adv. Ther.*, 2020, **3**, 2000024.
77 M. Martínez-Carmona and M. Vallet-Regí, *Nanomaterials*, 2020, **10**, 1443.
78 Z. Wang and F. G. Wu, *ChemNanoMat*, 2022, **8**, e202100369.
79 X. Zhai, B. Song, B. Chu, Y. Su, H. Wang and Y. He, *Nano Res.*, 2018, **11**, 6417–6427.
80 L. Zhang, X. Ji, Y. Su, X. Zhai, H. Xu, B. Song, A. Jiang, D. Guo and Y. He, *Nano Res.*, 2021, **14**, 52–58.
81 J. Tang, B. Chu, J. Wang, B. Song, Y. Su, H. Wang and Y. He, *Nat. Commun.*, 2019, **10**, 4057.
82 M. Cui, S. Liu, B. Song, D. Guo, J. Wang, G. Hu, Y. Su and Y. He, *Nano-Micro Lett.*, 2019, **11**, 73.
83 C. Song, Y. Zhong, X. Jiang, F. Peng, Y. Lu, X. Ji, Y. Su and Y. He, *Anal. Chem.*, 2015, **87**, 6718–6723.
84 M. Tang, X. Ji, H. Xu, L. Zhang, A. Jiang, B. Song, Y. Su and Y. He, *Anal. Chem.*, 2018, **90**, 8188–8195.
85 J. Xue, Z. Zhao, L. Zhang, L. Xue, S. Shen, Y. Wen, Z. Wei, L. Wang, L. Kong, H. Sun, Q. Ping, R. Mo and C. Zhang, *Nat. Nanotechnol.*, 2017, **12**, 692–700.
86 C. Gasca-Salas, B. Fernández-Rodríguez, J. A. Pineda-Pardo, R. Rodríguez-Rojas, I. Obeso, F. Hernández-Fernández, M. del Álamo, D. Mata, P. Guida, C. Ordás-Bandera, J. I. Montero-Roblas, R. Martínez-Fernández, G. Foffani, I. Rachmilevitch and J. A. Obeso, *Nat. Commun.*, 2021, **12**, 779.
87 L. P. Wu, D. Ahmadvand, J. Su, A. Hall, X. Tan, Z. S. Farhangrazi and S. M. Moghimi, *Nat. Commun.*, 2019, **10**, 4635.
88 K. S. Kim, *Nat. Rev. Microbiol.*, 2008, **6**, 625–634.
89 M. Coureuil, H. Lécuyer, S. Bourdoulous and X. Nassif, *Nat. Rev. Microbiol.*, 2017, **15**, 149–159.
90 Z. Fitzpatrick, G. Frazer, A. Ferro, S. Clare, N. Bouladoux, J. Ferdinand, Z. K. Tuong, M. L. Negro-Demontel, N. Kumar, O. Suchanek, T. Tajsic, K. Harcourt, K. Scott, R. Bashford-Rogers, A. Helmy, D. S. Reich, Y. Belkaid, T. D. Lawley, D. B. McGavern and M. R. Clatworthy, *Nature*, 2020, **587**, 472–476.
91 R. Sun, M. Liu, J. Lu, B. Chu, Y. Yang, B. Song, H. Wang and Y. He, *Nat. Commun.*, 2022, **13**, 5127.
92 B. Chu, Y. Yang, J. Tang, B. Song, Y. He and H. Wang, *Angew. Chem., Int. Ed.*, 2022, **61**, e202208422.
93 R. Sun, M. Liu, Z. Xu, B. Song, Y. He and H. Wang, *Nano Res.*, 2022, **15**, 7392–7401.
94 A. Jiang, B. Song, X. Ji, F. Peng, H. Wang, Y. Su and Y. He, *Nano Res.*, 2018, **11**, 2285–2294.
95 A. Narain, S. Asawa, V. Chhabria and Y. Patil-Sen, *Nanomedicine*, 2017, **12**, 2677–2692.
96 P. Gangadaran and B. C. Ahn, *Pharmaceutics*, 2020, **12**, 442.
97 J. Han, L. Zhang, M. Cui, Y. Su and Y. He, *Anal. Chem.*, 2021, **93**, 10122–10131.
98 Y. Jiang and K. Pu, *Chem. Rev.*, 2021, **121**, 13086–13131.
99 J. Wang, B. Song, J. Tang, G. Hu, J. Wang, M. Cui and Y. He, *Nano Res.*, 2020, **13**, 1614–1619.
100 M. Cui, M. Li, J. Wang, R. Chen, Z. Xu, J. Wang, J. Han, G. Hu, R. Sun, X. Jiang, B. Song and Y. He, *Angew. Chem., Int. Ed.*, 2021, **60**, 15490–15496.
101 M. Cui, P. Dai, J. Ding, M. Li, R. Sun, X. Jiang, M. Wu, X. Pang, M. Liu, Q. Zhao, B. Song and Y. He, *Angew. Chem., Int. Ed.*, 2022, **61**, e202200172.
102 X. Lin, J. Song, X. Chen and H. Yang, *Angew. Chem., Int. Ed.*, 2020, **59**, 14212–14233.
103 C. Pirri, C. Fede, L. Petrelli, D. Guidolin, C. Fan, R. De Caro and C. Stecco, *J. Anat.*, 2021, **238**, 999–1009.
104 L. Demi, T. Egan and M. Muller, *Appl. Sci.*, 2020, **10**, 462.
105 F. Darmoch, M. C. Alraies, Y. Al-Khadra, H. M. Pacha, D. S. Pinto and E. A. Osborn, *J. Am. Heart Assoc.*, 2020, **9**, e013678.
106 J. Cen, X. Ye, X. Liu, W. Pan, L. Zhang, G. Zhang, N. He, A. Shen, J. Hu and S. Liu, *Angew. Chem., Int. Ed.*, 2022, **61**, e202209610.
107 F. S. Foster, C. J. Pavlin, K. A. Harasiewicz, D. A. Christopher and D. H. Turnbull, *Ultrasound Med. Biol.*, 2000, **26**, 1–27.
108 E. G. Grant, C. B. Benson, G. L. Moneta, A. V. Alexandrov, J. D. Baker, E. I. Bluth, B. A. Carroll, M. Eliasziw, J. Gocke, B. S. Hertzberg, S. Katanick, L. Needleman, J. Pellerito, J. F. Polak, K. S. Rholl, D. L. Wooster and R. E. Zierler, *Radiology*, 2003, **229**, 340–346.
109 C. Demené, D. Maresca, M. Kohlhauer, F. Lidouren, P. Micheau, B. Ghaleh, M. Pernot, R. Tissier and M. Tanter, *Sci. Rep.*, 2018, **8**, 16436.
110 D. P. Sawyer, A. Bar-Zion, A. Farhadi, S. Shivaei, B. Ling, A. Lee-Gosselin and M. G. Shapiro, *Nat. Methods*, 2021, **18**, 945–952.
111 A. Ruland, K. J. Gilmore, L. Y. Daikuara, C. D. Fay, Z. Yue and G. G. Wallace, *Acta Biomater.*, 2019, **91**, 173–185.
112 E. Morokov, E. Khramtsova, E. Kuevda, E. Gubareva, T. Grigoriev, K. Lukanina and V. Levin, *Artif. Organs*, 2019, **43**, 1104–1110.
113 C. Rabut, M. Correia, V. Finel, S. Pezet, M. Pernot, T. Deffieux and M. Tanter, *Nat. Methods*, 2019, **16**, 994–997.
114 S. Noimark, R. J. Colchester, R. K. Poduval, E. Maneas, E. J. Alles, T. Zhao, E. Z. Zhang, M. Ashworth, E. Tsolaki, A. H. Chester, N. Latif, S. Bertazzo, A. L. David, S. Ourselin, P. C. Beard, I. P. Parkin, I. Papakonstantinou and A. E. Desjardins, *Adv. Funct. Mater.*, 2018, **28**, 1704919.
115 X. Qian, J. Pei, H. Zheng, X. Xie, L. Yan, H. Zhang, C. Han, X. Gao, H. Zhang, W. Zheng, Q. Sun, L. Lu and K. K. Shung, *Nat. Biomed. Eng.*, 2021, **5**, 522–532.

 This journal is © The Royal Society of Chemistry 2023

Published on 24 2023. Downloaded on 11/13/2025 12:52:34 PM.

116 J. Fang, Y. N. Ting and Y. W. Chen, *J. Ultrasound Med.*, 2022, **41**, 1699–1711.
117 A. Iula and A. Vizzuso, *Appl. Sci.*, 2022, **12**, 8285.
118 E. Naredo and I. Monteagudo, *Clin. Exp. Rheumatol.*, 2014, **32**, S12–19.
119 I. Tinazzi, D. McGonagle, P. Macchioni and S. Z. Aydin, *Rheumatology*, 2019, **59**, 2030–2034.
120 C. Martinoli, F. Pretolesi, G. Crespi, S. Bianchi, N. Gandolfo, M. Valle and L. E. Derchi, *Eur. J. Radiol.*, 1998, **27**, S133–S140.
121 V. L. Petrović, M. M. Janković, A. V. Lupšić, V. R. Mihajlović and J. S. Popović-Božović, *IEEE Access*, 2019, **7**, 74721–74733.
122 T. R. Skaug, B. H. Amundsen, T. Hergum, S. Urheim, H. Torp and B. O. Haugen, *Eur. Heart J. Cardiovasc. Imaging*, 2014, **15**, 615–622.
123 C. Yang, M. Guo, H. Liu, K. Yan, Y. J. Xu, H. Miao and Y. Fu, *Rev. Sci. Instrum.*, 2013, **84**, 121702.
124 K. Y. Leung and Y. L. Wan, *Life*, 2022, **12**, 226.
125 C. Demené, J. Mairesse, J. Baranger, M. Tanter and O. Baud, *NeuroImage*, 2019, **185**, 851–856.
126 S. B. Feinstein, B. Coll, D. Staub, D. Adam, A. F. L. Schinkel, F. J. ten Cate and K. Thomenius, *J. Nucl. Cardiol.*, 2010, **17**, 106–115.
127 Y. Zheng, L. Wang, X. Han, L. Shen, C. Ling, Z. Qian, L. Zhu, F. Dong and Q. Han, *Exp. Biol. Med.*, 2021, **247**, 97–105.
128 W. Wang, Y. Zheng, X. F. Wu, D. Zhao, L. Z. Hou, F. Shi, J. J. Liu and F. L. Dong, *Gland Surg.*, 2020, **9**, 1486–1494.
129 Y. Zheng, L. Bai, J. Sun, L. Zhu, R. Huang, S. Duan, F. Dong, Z. Tang and Y. Li, *Front. Oncol.*, 2022, **12**, 981106.
130 C. Chen, R. Perera, M. C. Kolios, H. Wijkstra, A. A. Exner, M. Mischi and S. Turco, *Sci. Rep.*, 2022, **12**, 13619.
131 A. Farhadi, G. H. Ho, D. P. Sawyer, R. W. Bourdeau and M. G. Shapiro, *Science*, 2019, **365**, 1469–1475.
132 A. de Leon, R. Perera, C. Hernandez, M. Cooley, O. Jung, S. Jeganathan, E. Abenojar, G. Fishbein, A. J. Sojahrood, C. C. Emerson, P. L. Stewart, M. C. Kolios and A. A. Exner, *Nanoscale*, 2019, **11**, 15647–15658.
133 R. Hou, X. Liang, X. Li, X. Zhang, X. Ma and F. Wang, *Biomater. Sci.*, 2020, **8**, 2526–2536.
134 L. Zhang, T. Yin, B. Li, R. Zheng, C. Qiu, K. S. Lam, Q. Zhang and X. Shuai, *ACS Nano*, 2018, **12**, 3449–3460.
135 L. Chen, S. F. Zhou, L. Su and J. Song, *ACS Nano*, 2019, **13**, 10887–10917.
136 I. C. Sun and S. Emelianov, *Nanoscale*, 2019, **11**, 16235–16240.
137 X. Lin, Y. Qiu, L. Song, S. Chen, X. Chen, G. Huang, J. Song, X. Chen and H. Yang, *Nanoscale Horiz.*, 2019, **4**, 747–756.
138 Q. Wu, Q. Zhang, T. Yu, X. Wang, C. Jia, Z. Zhao and J. Zhao, *ACS Appl. Bio Mater.*, 2021, **4**, 4244–4253.
139 Y. Wang, Y. Liu, J. E. Zhou, L. Lin, C. Jia, J. Wang, L. Yu, Y. Wang and Z. Yan, *Chem. Eng. J.*, 2021, **421**, 129917.
140 Y. Huang, K. Shen, Y. Si, C. Shan, H. Guo, M. Chen and L. Wu, *J. Colloid Interface Sci.*, 2021, **583**, 166–177.
141 K. H. Min, H. S. Min, H. J. Lee, D. J. Park, J. Y. Yhee, K. Kim, I. C. Kwon, S. Y. Jeong, O. F. Silvestre, X. Chen, Y. S. Hwang, E. C. Kim and S. C. Lee, *ACS Nano*, 2015, **9**, 134–145.
142 M. F. Chung, W. T. Chia, W. L. Wan, Y. J. Lin and H. W. Sung, *J. Am. Chem. Soc.*, 2015, **137**, 12462–12465.
143 K. Xu, Y. Cheng, J. Yan, Y. Feng, R. Zheng, X. Wu, Y. Wang, P. Song and H. Zhang, *Nano Res.*, 2019, **12**, 2947–2953.
144 C. J. Ke, W. L. Chiang, Z. X. Liao, H. L. Chen, P. S. Lai, J. S. Sun and H. W. Sung, *Biomaterials*, 2013, **34**, 1–10.
145 C. Huang, L. Zhang, Q. Guo, Y. Zuo, N. Wang, H. Wang, D. Kong, D. Zhu and L. Zhang, *Adv. Funct. Mater.*, 2021, **31**, 2010637.
146 E. Kang, H. S. Min, J. Lee, M. H. Han, H. J. Ahn, I. C. Yoon, K. Choi, K. Kim, K. Park and I. C. Kwon, *Angew. Chem., Int. Ed.*, 2010, **49**, 524–528.
147 S. Qi, P. Zhang, M. Ma, M. Yao, J. Wu, E. Mäkilä, J. Salonen, H. Ruskoaho, Y. Xu, H. A. Santos and H. Zhang, *Small*, 2019, **15**, 1804332.
148 L. V. Wang and S. Hu, *Science*, 2018, **335**, 1458–1462.
149 H. Ruan, Y. Liu, J. Xu, Y. Huang and C. Yang, *Nat. Photonics*, 2020, **14**, 511–516.
150 M. Xu and L. V. Wang, *Rev. Sci. Instrum.*, 2006, **77**, 041101.
151 A. G. Bell, *Am. J. Sci.*, 1880, **20**, 305.
152 L. Yang, J. Li, W. Pan, H. Wang, N. Li and B. Tang, *Chem. Commun.*, 2018, **54**, 3656–3659.
153 Z. Ye, P. K. Srivastava, Y. Xu, W. Wang, L. Jing, S. L. Chen and C. C. Tu, *ACS Appl. Nano Mater.*, 2019, **2**, 7577–7584.
154 Q. Fu, R. Zhu, J. Song, H. Yang and X. Chen, *Adv. Mater.*, 2019, **31**, 1805875.
155 Y. Liu, P. Bhattarai, Z. Dai and X. Chen, *Chem. Soc. Rev.*, 2019, **48**, 2053–2108.
156 Y. Mantri and J. V. Jokerst, *ACS Nano*, 2020, **14**, 9408–9422.
157 O. Santos, J. Cancino-Bernardi, P. M. Pincela Lins, D. Sampaio, T. Pavan and V. Zucolotto, *ACS Appl. Bio Mater.*, 2021, **4**, 6780–6790.
158 I. C. Sun, S. Jo, D. Dumani, W. S. Yun, H. Y. Yoon, D. K. Lim, C. H. Ahn, S. Emelianov and K. Kim, *Nanomaterials*, 2021, **11**, 1700.
159 E. Higbee-Dempsey, A. Amirshaghaghi, M. J. Case, J. Miller, T. M. Busch and A. Tsourkas, *Adv. Ther.*, 2019, **2**, 1900088.
160 T. Kim, Q. Zhang, J. Li, L. Zhang and J. V. Jokerst, *ACS Nano*, 2018, **12**, 5615–5625.
161 Y. Wang, Y. Yang, L. Yang, Y. Lin, Y. Tian, Q. Ni, S. Wang, H. Ju, J. Guo and G. Lu, *ACS Appl. Mater. Interfaces*, 2022, **14**, 28570–28580.
162 T. Repenko, A. Rix, A. Nedilko, J. Rose, A. Hermann, R. Vinokur, S. Moli, R. Cao-Milàn, M. Mayer, G. von Plessen, A. Fery, L. De Laporte, W. Lederle, D. N. Chigrin and A. J. C. Kuehne, *Adv. Funct. Mater.*, 2018, **28**, 1705607.
163 S. Raveendran, H. T. Lim, T. Maekawa, M. Vadakke Matham and D. Sakthi Kumar, *Nanoscale*, 2018, **10**, 13959–13968.
164 Y. Peng, Y. Liu, X. Lu, S. Wang, M. Chen, W. Huang, Z. Wu, G. Lu and L. Nie, *J. Mater. Chem. B*, 2018, **6**, 2813–2820.
165 S. Ye, G. Marston, J. R. McLaughlan, D. O. Sigle, N. Ingram, S. Freear, J. J. Baumberg, R. J. Bushby, A. F. Markham, K. Critchley, P. L. Coletta and S. D. Evans, *Adv. Funct. Mater.*, 2015, **25**, 2117–2127.
166 P. Ye, F. Li, J. Zou, Y. Luo, S. Wang, G. Lu, F. Zhang, C. Chen, J. Long, R. Jia, M. Shi, Y. Wang, X. Cheng, G. Ma and W. Wei, *Adv. Funct. Mater.*, 2022, **32**, 2110063.
167 L. Sun, Y. Chen, F. Gong, Q. Dang, G. Xiang, L. Cheng, F. Liao and M. Shao, *J. Mater. Chem. B*, 2019, **7**, 4393–4401.
168 R. Tian, L. Zhu, Z. Qin, G. Wang, J. Wang and H. Zhang, *Biomater. Sci.*, 2019, **7**, 5258–5269.
169 H. Moon, D. Kumar, H. Kim, C. Sim, J. H. Chang, J. M. Kim, H. Kim and D. K. Lim, *ACS Nano*, 2015, **9**, 2711–2719.
170 D. Peng, Y. Du, Y. Shi, D. Mao, X. Jia, H. Li, Y. Zhu, K. Wang and J. Tian, *Nanoscale*, 2016, **8**, 14480–14488.
171 X. Ge, B. Chen, T. Liu, L. Wei, L. Tong, Q. Ma, S. Gao and J. Song, *RSC Adv.*, 2019, **9**, 13494–13502.
172 E. N. Mueller, M. Kuriakose, S. Ganguly, K. Ma, M. A. Inzunza-Ibarra, T. W. Murray, J. N. Cha and A. P. Goodwin, *ACS Appl. Nano Mater.*, 2021, **4**, 12073–12082.
173 Y. Chen, C. Xu, Y. Cheng and Q. Cheng, *Photoacoustics*, 2021, **23**, 100284.
174 Y. Liu, X. Dai, B. Yu, M. Chen, N. Zhao and F. J. Xu, *Biomater. Sci.*, 2022, **10**, 2618–2627.
175 C. Yang, W. Jiang, Y. Yu, H. Zhang, C. Cai and Q. Shen, *J. Mater. Chem. B*, 2022, **10**, 2028–2037.
176 Y. Mantri, I. Sit, J. Zhou, V. H. Grassian and J. V. Jokerst, *J. Phys. Chem. C*, 2022, **126**, 7605–7614.
177 V. P. Nguyen, W. Qian, Y. Li, B. Liu, M. Aaberg, J. Henry, W. Zhang, X. Wang and Y. M. Paulus, *Nat. Commun.*, 2021, **12**, 34.
178 V. P. Nguyen, W. Fan, T. Zhu, W. Qian, Y. Li, B. Liu, W. Zhang, J. Henry, S. Yuan, X. Wang and Y. M. Paulus, *ACS Nano*, 2021, **15**, 13289–13306.
179 C. Zhou, L. Zhang, T. Sun, Y. Zhang, Y. Liu, M. Gong, Z. Xu, M. Du, Y. Liu, G. Liu and D. Zhang, *Adv. Mater.*, 2021, **33**, 2006532.
180 T. Chen, L. Su, L. Lin, X. Ge, F. Bai, M. Niu, C. Wang, J. Song, S. Guo and H. Yang, *Nano Res.*, 2022, **15**, 4154–4163.
181 N. Lv, X. Zhang, S. Wang, Y. Wu, X. Ge, J. Song, Q. Ma and S. Gao, *Adv. Opt. Mater.*, 2022, **10**, 2200694.
182 T. Chen, L. Su, X. Ge, W. Zhang, Q. Li, X. Zhang, J. Ye, L. Lin, J. Song and H. Yang, *Nano Res.*, 2020, **13**, 3268–3277.
183 Y. S. Chen, S. J. Yoon, W. Frey, M. Dockery and S. Emelianov, *Nat. Commun.*, 2017, **8**, 15782.
184 D. Zheng, K. Zhang, B. Chen, N. Zhao and F. J. Xu, *Small*, 2020, **16**, 2002790.
185 D. S. Dumani, I. C. Sun and S. Y. Emelianov, *Nanoscale*, 2019, **11**, 11649–11659.
186 H. Wang, L. An, C. Tao, Z. Ling, J. Lin, Q. Tian and S. Yang, *Nanoscale*, 2020, **12**, 5139–5150.
187 D. Liu, L. Liu, F. Liu, M. Zhang, P. Wei and T. Yi, *Adv. Sci.*, 2021, **8**, 2100074.

188 R. Zhang, L. Wang, X. Wang, Q. Jia, Z. Chen, Z. Yang, R. Ji, J. Tian and Z. Wang, *Adv. Healthcare Mater.*, 2020, **9**, 2000394.
189 M. Yuan, X. Fang, Y. Wu, Y. Xu, H. Feng, J. Mu, Z. Chen, Y. Lin, Q. Fu, W. Du, H. Yang and J. Song, *Anal. Chem.*, 2022, **94**, 5204–5211.
190 Y. Yang, B. Chu, J. Cheng, J. Tang, B. Song, H. Wang and Y. He, *Nat. Commun.*, 2022, **13**, 1255.
191 Q. Mao, J. Fang, A. Wang, Y. Zhang, C. Cui, S. Ye, Y. Zhao, Y. Feng, J. Li and H. Shi, *Angew. Chem., Int. Ed.*, 2021, **60**, 23805–23811.
192 X. Cheng, R. Sun, L. Yin, Z. Chai, H. Shi and M. Gao, *Adv. Mater.*, 2017, **29**, 1604894.
193 S. Hong, D. W. Zheng, C. Zhang, Q. X. Huang, S. X. Cheng and X. Z. Zhang, *Sci. Adv.*, 2020, **6**, eabb0020.

Published on 24 2023. Downloaded on 11/13/2025 12:52:34 PM.

 This journal is © The Royal Society of Chemistry 2023